

2-Methylthio-imidazolins: a rare case of different tautomeric forms in solid state and in solution

Venelin Enchev, Nadezhda Markova, Marin Marinov, Neyko Stoyanov, Marin Rogojerov, Angel Ugrinov, Iwona Wawer & Dariusz Maciej Pisklak

Structural Chemistry

Computational and Experimental
Studies of Chemical and Biological
Systems

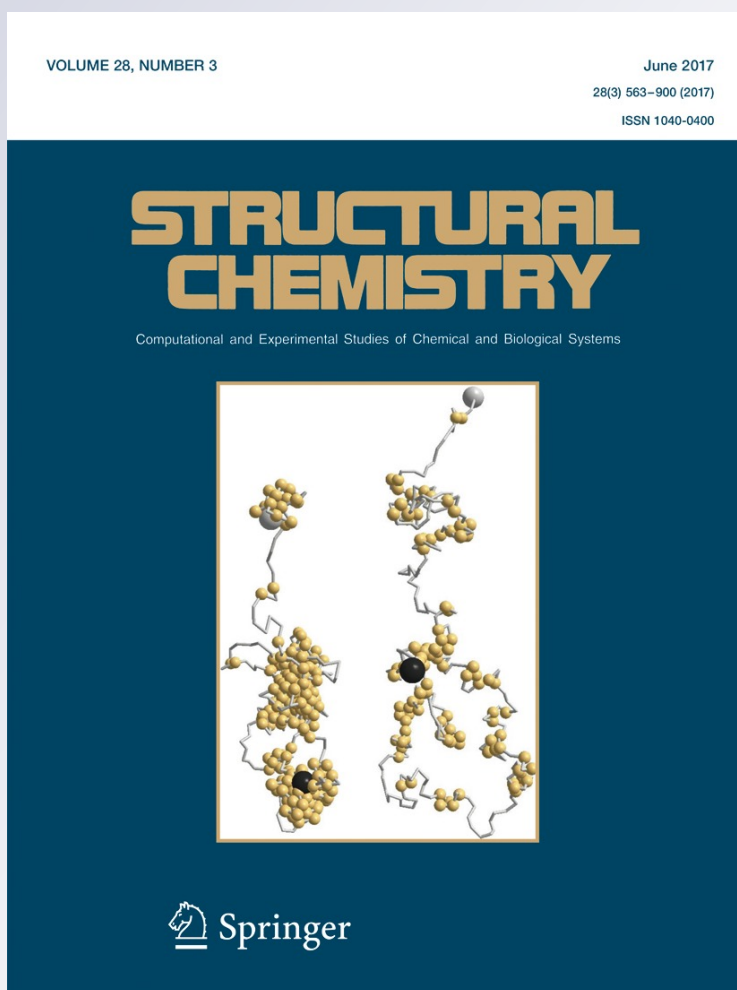
ISSN 1040-0400

Volume 28

Number 3

Struct Chem (2017) 28:757–772

DOI 10.1007/s11224-016-0860-4



Your article is protected by copyright and all rights are held exclusively by Springer Science +Business Media New York. This e-offprint is for personal use only and shall not be self-archived in electronic repositories. If you wish to self-archive your article, please use the accepted manuscript version for posting on your own website. You may further deposit the accepted manuscript version in any repository, provided it is only made publicly available 12 months after official publication or later and provided acknowledgement is given to the original source of publication and a link is inserted to the published article on Springer's website. The link must be accompanied by the following text: "The final publication is available at link.springer.com".

2-Methylthio-imidazolins: a rare case of different tautomeric forms in solid state and in solution

Venelin Enchev¹ · Nadezhda Markova¹ · Marin Marinov² · Neyko Stoyanov³ ·
 Marin Rogojerov¹ · Angel Ugrinov⁴ · Iwona Wawer⁵ · Dariusz Maciej Pisklak⁵

Received: 18 August 2016 / Accepted: 30 September 2016 / Published online: 14 October 2016
 © Springer Science+Business Media New York 2016

Abstract The synthesis and structure elucidation of two new compounds, 2-(methylthio)-1,3-diazaspiro[4.4]non-2-ene-4-one (**1**) and 2-(methylthio)-1,3-diazaspiro[4.4]non-2-ene-4-thione (**2**), are presented. Both compounds crystallized in monoclinic crystal system. Compound **1** formed plate-like colorless crystals, while compound **2** gave yellow needles. The structural and spectral characteristics of both compounds are studied by IR and NMR spectroscopy and quantum chemistry. The optimized geometry, harmonic vibrational frequencies, and NMR shielding are calculated by DFT employing B3LYP functional using 6-311++G(*d,p*) basis set. Our results support the hydrogen bonding pattern observed in reported crystalline structure. Evidences are given indicating that the tautomeric form in solution is different from that one in solid state. The substantial difference between positions of the characteristic

C=N band in nonpolar solvent and crystalline phase for both compounds suggests that in solid state a “conjugated tautomeric form” exists, while in solution phase there is “non-conjugated tautomeric form”. In polar solvents, both tautomeric forms exist. It is suggested to call this phenomenon *desmokatastropy*—from Greeks δεσμός (bond) κατάστασις (state) and τρόπος (change).

Keywords Tautomerism · 2-methylthio-imidazolins · Solid state · Solvent effect · DFT

Introduction

At the end of nineteenth century, it was known the dualistic behavior of ethyl acetoacetate, discovered in 1863 by Geuther [1], in chemical reactions. With some substances, it acts as compound contained a hydroxyl group, while with other ones as a ketonic compound. In 1882, Baeyer and Oekonomides [2] found out that isatin gives two isomeric *N*- and *O*-methyl derivatives. Baeyer explained this fact with *pseudomerie* [3]—the possibility of one compound to have more than one structure. In 1885 Laar [4] defined these systems as triadic (HX–Y=Z and X=Y–ZH) and postulates that they cannot be separated experimentally. He proposed to call this phenomenon *tautomerism* (ταυτό—identity, μέρος—part). Two years later, in an attempt to improve the hypothesis deduced by Laar, Jacobson [5] introduced the term *desmotropy* (δεσμός—bond, τρόπος—change). To differentiate between *tautomerism* and *desmotropy*, Hantzsch and Hermann [6] suggested that if a substance could be isolated in two stable forms, it should be called *desmotropic*, while if it could not be isolated, it should be termed *tautomeric*. In 1896 Claisen [7] isolated acetyldibenzoylmethane as two separate solid-state forms—enol and keto forms, each with different

Electronic supplementary material The online version of this article (doi:10.1007/s11224-016-0860-4) contains supplementary material, which is available to authorized users.

✉ Venelin Enchev
 venelin@orgchm.bas.bg

- ¹ Institute of Organic Chemistry, Bulgarian Academy of Sciences, 1113 Sofia, Bulgaria
- ² Faculty of Plant Protection and Agroecology, Department of General Chemistry, Agricultural University – Plovdiv, Plovdiv, Bulgaria
- ³ Department of Chemistry and Chemical Technology, University of Ruse – Razgrad Branch, 47 Aprilsko Vastanie Blvd, 7200 Razgrad, Bulgaria
- ⁴ Department of Chemistry and Biochemistry, North Dakota State University, 1231 Albrecht Blvd, Fargo, ND 58102, USA
- ⁵ Faculty of Pharmacy, Medical University of Warsaw, Banacha 1, 02097 Warsaw, Poland

melting point and chemical properties. The keto and enol forms could be isolated from any mixtures which they formed: both heated in a solvent such as alcohol, or fused in the absence of solvents. In this way the existence of the desmotropic forms has been proven to be correct.

According to early reviews [8, 9], tautomerism was considered as an equilibrium between forms coexisting in solution. Comparison between experimental data obtained for mixture of tautomers and the alkyl derivatives of the respective tautomeric forms, so-called *fixed tautomers* [10, 11], was found to be helpful to study tautomerism. The term *desmotropy* was defined as *tautomerism in which both tautomeric forms have been isolated* [12], and its corresponds to the solid state.

The observation of different tautomers in the solid state is a rare phenomenon [13]. In 2011 Cruz-Cabeza and Groom [14] carried out a survey of the Cambridge Structural Database (CSD) concerning the identification, classification, and relative stability of tautomers. They identified 108 molecules that crystallize in two different tautomeric forms which represents just 0.05 % of the molecules in the CSD. The majority of observed pairs of tautomers have small energy differences of less than 12 kJ mol^{-1} according to calculations at B3LYP/6-311++G(d,p) level, and Cruz-Cabeza and Groom made a general rule that for two tautomers to be observed in the solid state, their relative energy must not exceed that of a strong hydrogen bond typical for organic crystals [14].

Pairs of tautomers also might coexist in a single crystal [15–22]. Among the crystal structures containing two tautomers can find ordered crystal structures with varying stoichiometric ratios of tautomers [19–21] and structures showing disorder between the two tautomeric forms [22]. A very rare case in which both tautomers quickly interconvert from one to another in crystal was observed by Enchev et al. [23]. Unique cases displaying both desmotropy and polymorphism were published recently [24–26].

Physical property measurements may be less accurate for molecules that can tautomerize. The different tautomers of the molecule usually have different properties [27]. According to Faller and Ertl [28] the main reason for inaccurate calculation of hydrophobicity, $\log p$, is the use of incorrect tautomeric forms of structures in the calculations. Because of *tautomeric problem*, some of drug-like structures may exist in dozen of tautomeric forms, energetically quite close. In some cases the form present in the solid state (and therefore used for calculation of properties) does not correspond to the form present in the solution. For example, there is evidence indicating that in aqueous solution, the product formed between diethyl aminomalonate and pyridoxal is the Schiff base, and not the 1,4-dihydropyridine tautomer which exists in the solid state [29].

In 1964 Lempert et al. [30] reported case of desmotropic forms for S-methylated 2-thiohydantoin. They obtained two tautomers of 2-methylthio-4,4/5,5/-diphenyl-2-imidazolin-5(4)-one whose structure assignments were based on their IR spectra by using different procedures of recrystallization. The “conjugated” form has been obtained on recrystallization from ethanol or ethanol pyridine mixtures while the “non-conjugated form”—either by recrystallization from chloroform and light petroleum or by sublimation at reduced pressure. Final proof for the separate existence of the two individual desmotropic forms has been obtained by X-ray determination of the crystal and molecular structure of these compounds [31]. The desmotropic forms have been found to be completely stable in the crystalline state, both being unchanged for periods of at several years [31].

Here we present our results on the synthesis and structure of new compounds obtained by methylated of the sulfur atom in cyclopentanespiro-5-(2-thiohydantoin) and cyclopentanespiro-5-(2,4-dithiohydantoin) and relative stability of the tautomers. Evidence is presented indicating that the tautomeric form in solution is different from that one in solid state.

Experimental and computational details

Synthesis of 2-methylthio-imidazolins

A mixture of cyclopentanespiro-5-(2-thiohydantoin) or cyclopentanespiro-5-(2,4-dithiohydantoin) (10 mmol), boron trifluoride dimethyl etherate (3.6 ml, 40 mmol), and toluene (30 ml) is refluxed for 12 h. After cooling the resulting crystalline product 2-(methylthio)-1,3-diazaspiro[4.4]non-2-ene-4-one (**1**) or 2-(methylthio)-1,3-diazaspiro[4.4]non-2-ene-4-thione (**2**) is filtered off and treated with triethylamine (6 ml, 43 mmol) in dichloromethane (20 ml). The solvent is evaporated in vacuum, and the product obtained is recrystallized from acetonitrile. 2-(Methylthio)-1,3-diazaspiro[4.4]non-2-ene-4-one: yield 74.93 %, m.p. 172–173 °C; 2-(methylthio)-1,3-diazaspiro[4.4]non-2-ene-4-thione: yield 91.30 %, m.p. 130–131 °C.

Infrared spectra

Solid-state IR spectra were recorded on FTIR spectrometer Bruker *Tensor 27* in the $3500\text{--}550 \text{ cm}^{-1}$ spectral region with resolution of 2 cm^{-1} using ATR appliance—Pike Miracle with ZnSe crystal plate. The IR spectra of saturated solutions of both compounds in CCl_4 and dry ethanol (100 %) were measured in a 1 mm KBr liquid cell and 0.2 mm CaF liquid cell, respectively.

Table 1 Crystal and refinement parameters for compounds **1** and **2**

| Parameters | 1A | 2A |
|--------------------------------------------------------------|-----------------------------------------------------------------|-----------------------------------------------------------------|
| Empirical formula | C ₈ H ₁₂ N ₂ OS | C ₈ H ₁₂ N ₂ S ₂ |
| Formula weight | 184.26 | 200.32 |
| Temperature/K | 100 (2) | 100 (2) |
| Crystal system | Monoclinic | Monoclinic |
| Space group | P2 ₁ /c | P2 ₁ /c |
| <i>a</i> /Å | 9.6084(4) | 7.2041(3) |
| <i>b</i> /Å | 10.3444(4) | 14.2278(5) |
| <i>c</i> /Å | 9.7529(5) | 9.7725(4) |
| α /° | 90.00 | 90.00 |
| β /° | 114.205(3) | 103.236(3) |
| γ /° | 90.00 | 90.00 |
| Volume/Å ³ | 884.15(7) | 975.06(7) |
| <i>Z</i> | 4 | 4 |
| ρ_{calc} mg/mm ³ | 1.384 | 1.365 |
| μ /mm ^{−1} | 2.871 | 4.518 |
| <i>F</i> (000) | 392.0 | 424.0 |
| Crystal size/mm ³ | 0.21 × 0.1 × 0.01 | 0.31 × 0.05 × 0.01 |
| 2 θ range for data collection | 10.1°–133.14° | 11.18°–136.22° |
| Index ranges | −11 ≤ <i>h</i> ≤ 10, −12 ≤ <i>k</i> ≤ 12, −9 ≤ <i>l</i> ≤ 11 | −8 ≤ <i>h</i> ≤ 8, −16 ≤ <i>k</i> ≤ 17, −11 ≤ <i>l</i> ≤ 9 |
| Reflections collected | 10,191 | 12,590 |
| Independent reflections | 1567[R(int) = 0.0851] | 1760[R(int) = 0.0598] |
| Data/restraints/parameters | 1567/0/114 | 1760/0/114 |
| Goodness of fit on <i>F</i> ² | 1.145 | 1.055 |
| Final <i>R</i> indexes [<i>I</i> ≥ 2 σ (<i>I</i>)] | <i>R</i> ₁ = 0.0368, <i>wR</i> ₂ = 0.0823 | <i>R</i> ₁ = 0.0394, <i>wR</i> ₂ = 0.0955 |
| Final <i>R</i> indexes (all data) | <i>R</i> ₁ = 0.0591, <i>wR</i> ₂ = 0.1044 | <i>R</i> ₁ = 0.0485, <i>wR</i> ₂ = 0.1008 |
| Largest diff. peak/hole/e Å ^{−3} | 0.42/−0.45 | 0.43/−0.32 |

$R_1 = \Sigma ||F_o| - |F_c|| / \Sigma |F_o|$, $wR_2 = [\Sigma w[(F_o)^2 - (F_c)^2]^2 / \Sigma w(F_o)^2]^{1/2}$ for $F_o > 2\sigma(F_o)$, $w = [\sigma^2(F_o)^2 + (AP)^2 + BP]^{-1}$ where $P = [(F_o)^2 + 2(F_c)^2]/3$ and *A*, *B* coefficients for both compounds as follow: 1A, *A* (*B*) = 0.0389 (0.8315); 2A, *A* (*B*) = 0.0548 (0.7108)

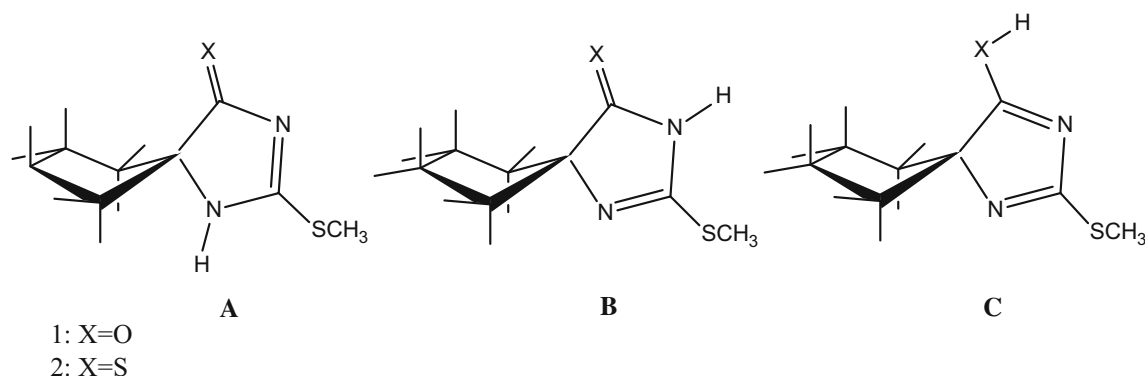


Fig. 1 Possible tautomers of 2-(methylthio)-1,3-diazaspiro[4.4]non-2-ene-4-one (**1**) and 2-(methylthio)-1,3-diazaspiro[4.4]non-2-ene-4-thione (**2**)

Solid-state NMR

The solid-state ¹³C cross-polarization (CP) magic angle spinning (MAS) spectra were recorded on a Bruker DRX-400 spectrometer at 100.61 MHz. The powder samples

were spun at 10 kHz in a 4-mm ZrO₂ rotor (contact time of 2 ms, repetition time of 6 s), and 600 scans were accumulated. ¹³C chemical shifts were calibrated indirectly (external reference) through the glycine CO signal recorded at 176.0 ppm relative to TMS. For ¹⁵N MAS spectra a

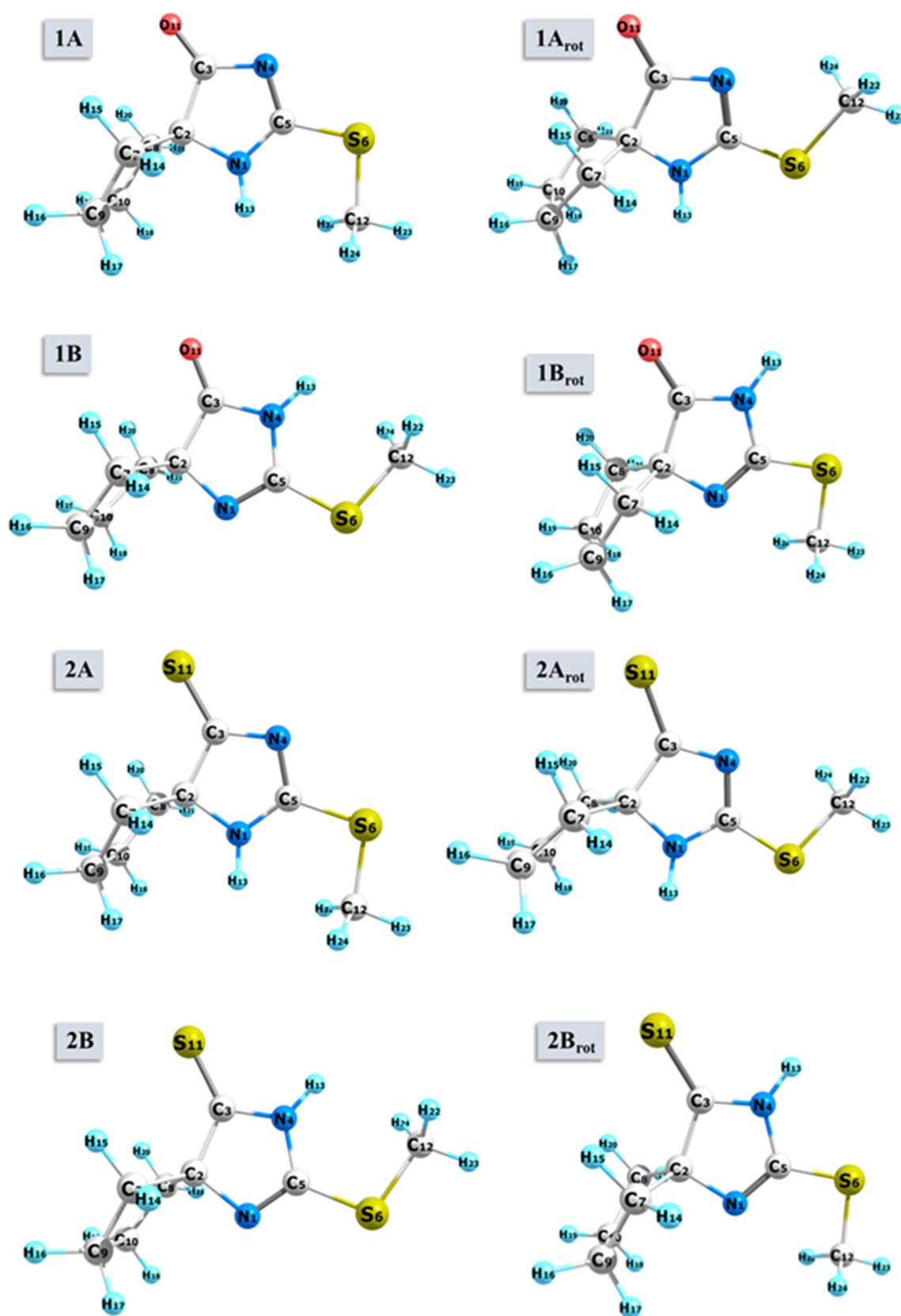


Fig. 2 B3LYP/6-311++G(d,p) optimized structures of tautomers **A** and **B**, and their rotamers **A_{rot}** and **B_{rot}** of 2-(methylthio)-1,3-diazaspiro[4.4]non-2-ene-4-one (**1**) and 2-(methylthio)-1,3-diazaspiro[4.4]non-2-ene-4-thione (**2**)

Table 2 B3LYP/6-311++G(*d,p*) calculated Gibbs free energy differences, ΔG_{298} (kcal mol⁻¹) and populations (in %) for the tautomers **A–C** of the compounds shown on Fig. 1

| Tautomer | Gas phase | | Solution | | | | | | | |
|-------------------------|------------------|----------------------|------------------|-----------------------|-------------------|-----------------------|-----------------------------------|----------------------|------------------|----------------------|
| | | | CCl ₄ | | CHCl ₃ | | CH ₃ COCH ₃ | | EtOH | |
| | ΔG_{298} | Popul. | ΔG_{298} | Popul. | ΔG_{298} | Popul. | ΔG_{298} | Popul. | ΔG_{298} | Popul. |
| 1A | 6.55 | 1.6×10^{-3} | 2.62 | 1.13 | 0.41 | 30.39 | 0.00 | 55.35 | 0.00 | 62.08 |
| 1A_{rot} | 3.11 | 0.52 | 1.89 | 3.87 | 1.17 | 8.43 | 0.77 | 15.15 | 0.95 | 13.29 |
| 1B | 3.96 | 0.12 | 2.73 | 0.93 | 2.88 | 0.47 | 3.21 | 0.24 | 3.35 | 0.23 |
| 1B_{rot} | 0.00 | 99.35 | 0.00 | 94.06 | 0.00 | 60.71 | 0.38 | 29.26 | 0.59 | 24.40 |
| 1C | 13.94 | 6.0×10^{-9} | 12.49 | 6.57×10^{-8} | 13.49 | 1.29×10^{-8} | 14.09 | 2.6×10^{-9} | 14.24 | 2.4×10^{-9} |
| 2A | 7.77 | 2.0×10^{-6} | 2.47 | 1.31 | 0.48 | 18.11 | 0.00 | 53.33 | 0.00 | 57.50 |
| 2A_{rot} | 4.35 | 0.06 | 1.38 | 8.26 | 0.18 | 31.92 | 0.22 | 36.79 | 0.32 | 33.50 |
| 2B | 3.19 | 0.46 | 1.61 | 5.60 | 1.15 | 5.11 | 1.92 | 2.09 | 1.89 | 2.37 |
| 2B_{rot} | 0.00 | 99.48 | 0.00 | 84.82 | 0.00 | 44.85 | 1.14 | 7.78 | 1.28 | 6.63 |
| 2C | 9.56 | 9.7×10^{-6} | 10.45 | 2.18×10^{-6} | 10.72 | 4.0×10^{-8} | 12.01 | 5.3×10^{-8} | 12.19 | 5.7×10^{-8} |

For the rotamers see Fig. 2

contact time of 7 ms, repetition time of 8 ms, and spectral width of 32 kHz were used, and ca. 8000 scans were accumulated. The chemical shifts were calibrated on the nitromethane scale through the glycine NH signal at –347.6 ppm.

Single-crystal X-ray analysis

In order to prepare high-quality crystals suitable for single-crystal X-ray data collection, few crystals of compounds **1** and **2** were dissolved in different vials in a minimum amount of acetone. Both vials were capped with rubber septa stuck with a needle and left undisturbed in the hood. Compound **1** formed plate-like colorless crystals, while compound **2** gave yellow needles.

Bruker Apex2 Duo diffractometer with CCD area detector, four-circle goniometer, and I μ S Cu X-ray radiation was used to collect the data at T = 100 K. Both structures were processed with Apex2 v2010.9-1 software package (SAINT v. 7.68A) and solved with direct method. Olex2 software [32], was used for structures refinement and final preparation for publication. Details of data collection and refinement are given in Table 1.

Quantum chemical calculations

The optimization of the structure for the tautomers of compounds **1** and **2** shown in Fig. 1 was carried out at B3LYP/6-311++G(*d,p*) computational level using the GAMESS package [33, 34]. The default gradient convergence threshold (1×10^{-4} hartree Bohr⁻¹) was used. Frequency calculations at the same level of theory were carried out to confirm that the obtained structures

correspond to energy minima. To estimate the effect of the medium (CCl₄, CHCl₃, CH₃COCH₃, and C₂H₅OH) on the relative stabilities of the tautomers of **1** and **2**, all of the stationary point geometries were fully optimized again in the reaction field of the implicit solvent at the same computational level. Solution-phase vibrational frequencies were computed for each stationary point on the basis of numerical Hessians. Solvent effect was accounted by using the self-consistent reaction field (SCRF) method with the conductor polarizable continuum model (C-PCM) formalism [35]. In this model, the molecule is embedded in a cavity surrounded by an infinite dielectric which approximates the solvent as a structureless polarizable continuum characterized by its macroscopic dielectric permittivity. We applied the conductor polarizable continuum model as implemented in GAMESS [33, 34].

In order to examine the effects of hydrogen bonding, one dimer model of tautomer **B** and one trimer model of tautomer **A** were constructed. The structures of dimers of tautomer **B** (Fig. 1) were optimized in gas phase and in CCl₄ and C₂H₅OH solution phase, and the structures of trimers of tautomer **A** were optimized in gas phase to explain the changes in observed IR frequencies and XRD data for compound **1** and **2**. The interaction energies may be affected by the basis set superposition error (BSSE) which is usually corrected by the method of Boys and Bernardi [36]. However, a moderately large basis sets, 6-311++G(*d,p*), is used and the BSSE will not significantly affect the results in our study.

The values of Gibbs free energies in gas phase and in solution phase were calculated at temperature of 298.15 K. The values of the populations (p_i) were calculated by the standard formula: $p_i = e^{-\Delta G_i/RT} / \sum_i e^{-\Delta G_i/RT}$.

The NMR chemical shieldings were calculated at B3LYP/6-311+G(2df,p) level using the GIAO (gauge-including atomic orbitals) approach and B3LYP/6-311++G(d,p) optimized geometry. In order to compare with experiment, the calculated absolute shieldings were transformed to chemical shifts using as reference compounds nitromethane for nitrogen atoms (-154.547) and tetramethylsilane for carbon atoms (183.133): $\delta = \delta_{\text{calc}}(\text{reference}) - \delta_{\text{calc}}$. Both $\delta_{\text{calc}}(\text{reference})$ and δ_{calc} were evaluated with the same method and basis set. The NMR calculations were carried out using Gaussian 09 [37].

Results and discussion

The newly synthesized compounds, 2-(methylthio)-1,3-diazaspiro[4.4]non-2-ene-4-one, **1**, and 2-(methylthio)-1,3-diazaspiro[4.4]non-2-ene-4-thione, **2**, described in “[Synthesis of 2-methylthio-imidazolins](#)” section may theoretically exist in three tautomeric forms, **A–C**, shown in Fig. 1. In addition each of the tautomers **A** and **B** may also exist in two rotamers presented in Fig. 2.

Tautomeric equilibrium in different solvents

After optimization at B3LYP/6-311++G(d,p) level of the structures of all tautomers and possible rotamers of both compounds, tautomer **B_{rot}** was found to be the most stable in the gas phase. Its quantity, according to the calculated relative stabilities, amounts to 99.35 % for **1** and 99.48 % for **2** (Table 2).

The rotamer **1B_{rot}** is also most stable in CCl₄ and CHCl₃ solution. However, its fraction decreases to 94.06 % in CCl₄ and 60.71 % in CHCl₃. The calculated populations of **1A** and **1A_{rot}** in CCl₄ increase to 1.13 and 3.87 %, respectively. In solvent CHCl₃ the populations were calculated to be **1B_{rot}**: **1A**: **1A_{rot}** = 60.71: 30.39: 8.43 %. The similar tendency is observed for 2-methylthio-5-cyclopentanespiro-2-imidazolin-4-thion, **2**, in CCl₄ (Table 2). In CHCl₃, however, the amount of **2A_{rot}** prevails over **2A** and the ratio is—**2B_{rot}**: **2A**: **2A_{rot}** = 44.85: 18.11: 31.92 %.

Going from nonpolar or weak-polar to polar solvents, the energy difference between the tautomers and rotamers of **A** and **B** changes, and in acetone and ethanol the structure **A** becomes the most stable (Table 2).

The population of tautomer **1A** and its rotamer **1A_{rot}** in acetone solution is 55.35 and 15.15 %, respectively. The amount of **1B_{rot}** decreases to 29.26 %. In ethanol this proportion is **1A**: **1A_{rot}**: **1B_{rot}** = 62.08: 13.29: 24.40 %.

For compound **2**, the populations in acetone are **2A**: **2A_{rot}**: **2B_{rot}** = 53.33: 36.79: 7.78 %, while in ethanol this ratio is 57.50: 33.50: 6.63 %. A minor fraction of the form

Table 3 Selected frequency data calculated at B3LYP/6-311++G(d,p) level for tautomer **A** and its trimer of compounds **1** and **2** (Fig. 1)

| Calculated | Experimental ^a | | | | | | Assignment |
|-------------------------|---------------------------|------------|------------------|------------------|------------------|------------------|------------------------------|
| | 1A | | | 1A trimer | | | |
| | Gas | EtOH | CCl ₄ | Gas | CCl ₄ | EtOH | |
| 1A_{rot} | | | | | | | |
| Gas | | | | | | | |
| 3646 (35) | 3668 (67) | 3661 (110) | 3652 (24) | 3663 (55) | 3663 (106) | 3445 (47) | ν(N1-H) |
| 1793 (337) | 1761 (490) | 1728 (672) | 1792 (369) | 1760 (538) | 1718 (735) | 1765 (335) | ν(C=O) + ν(C2-C3) + ν(C3-N4) |
| 1515 (421) | 1507 (537) | 1462 (606) | 1513 (493) | 1474 (619) | 1439 (940) | 1461 (697) | ν(C=N) + δ(N1-H) |
| 1449 (248) | 1476 (365) | 1487 (559) | 1438 (208) | 1460 (288) | 1473 (431) | 1470 (87) | δ(N1-H) |
| 2A_{rot} | | | | | | 2A trimer | |
| 3660 (54) | 3649 (110) | 3651 (195) | 3670 (41) | 3675 (91) | 3669 (160) | 3422 (611) | ν(N1-H) |
| 1459 (181) | 1509 (360) | 1514 (472) | 1458 (246) | 1491 (355) | 1505 (435) | 1522 (163) | ν(C-N) + δ(N1-H) |
| 1474 (148) | 1452 (195) | 1436 (224) | 1470 (43) | 1440 (454) | 1420 (325) | 1435 (244) | δ(N1-H) + ν(C=N) |
| 1291 (682) | 1279 (1170) | 1264 (99) | 1294 (747) | 1282 (705) | 1276 (1793) | 1299 (63) | ν(C=S) |

The frequencies are in cm⁻¹ and intensities (in brackets) in km mol⁻¹

^a Solid state

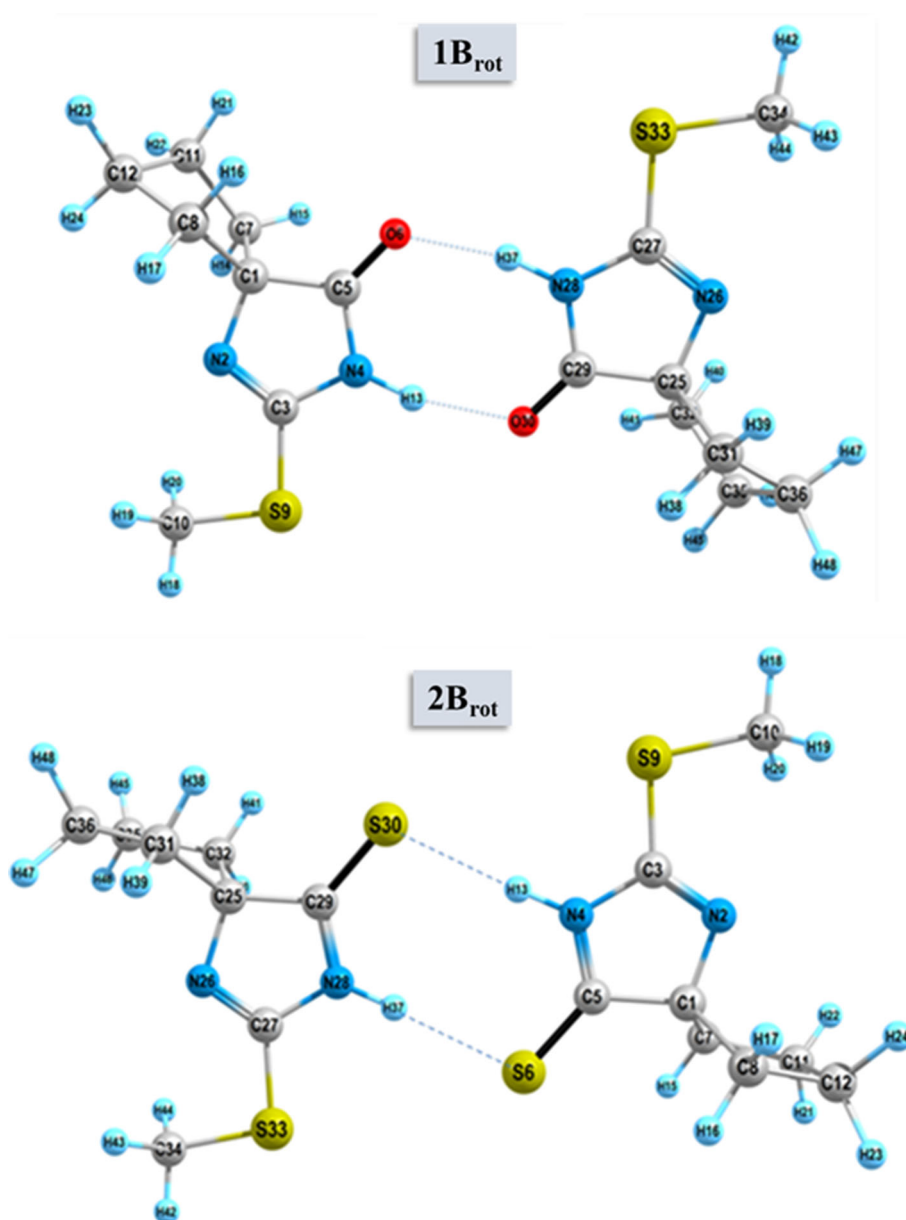
Table 4 Selected frequency data calculated at B3LYP/6-311++G(d,p) level for tautomer **B** and its dimer of compounds **1** and **2** (Fig. 1)

| Calculated | | | | | | | | | | Experimental ^a | Assignment | | |
|-------------------|------------------|------------|------------|--------------------------|------------|-------------|-------------|------------------|------------|---------------------------|------------|-----------------|--------------------------------------------------------------------|
| 1B _{rot} | | | | 1 B _{rot} dimer | | | | CCl ₄ | EtOH | | | | |
| Gas | CCl ₄ | EtOH | Gas | CCl ₄ | EtOH | Gas | | | | | | | |
| 3653 (50) | 3648 (83) | 3634 (127) | 3610 (62) | 3604 (94) | 3602 (131) | 3313 (2147) | 3259 (320) | 3289 (2788) | 3256 (8) | 3307 (2439) | 3272 (391) | 3435 low inten. | $\nu_{as}(\text{N-H}\dots\text{O}=\text{C})^b$ |
| 1804 (421) | 1782 (609) | 1758 (832) | 1806 (452) | 1777 (660) | 1747 (911) | 1764 (1150) | 1740 (0.2) | 1750(1497) | | 1730 (1866) | 1721 (20) | 1753 | $\nu_{as}(\text{C}=\text{O}\dots\text{H-N}) + \delta(\text{N-H})$ |
| 1627 (349) | 1621 (454) | 1611 (568) | 1625 (275) | 1619 (368) | 1613 (478) | 1619 (466) | | 1616 (542) | | 1610 (72) | 1605 (138) | 1723 | $\nu_s(\text{C}=\text{O}\dots\text{H-N}) + \delta(\text{N-H})$ |
| 1398 (158) | 1426 (157) | 1427 (188) | 1407 (171) | 1447 (161) | 1456 (186) | 1472 (13) | | 1612 (97) | | 1509 (50) | 1504 (11) | 1579 | $\nu_{as}(\text{C}=\text{N}) \nu_s(\text{C}=\text{N})$ |
| | | | | | | | | 1519 (128) | | 1509 (50) | 1504 (11) | 1373 | $\delta(\text{N4-H})$ |
| | | | | | | | | 1484 (266) | | | | | |
| 2B _{rot} | | | | | | | | | | | | | |
| 3634 (46) | 3613 (80) | 3605 (122) | 3592 (55) | 3588 (91) | 3575 (139) | 3284 (2510) | 3249 (0.01) | 3244 (2630) | 3194 (608) | 3246 (2704) | 3201 (906) | 3418 | $\nu_s(\text{N-H}\dots\text{S}=\text{C})^b$ |
| 1632 (294) | 1624 (362) | 1618 (495) | 1631 (259) | 1631 (367) | 1626 (502) | 1634 (485) | 1632 (0.00) | 1639 (726) | 1636 (27) | 1634 (899) | 1632 (149) | Low inten. | $\nu_{as}(\text{N-H}\dots\text{S}=\text{C})^b$ |
| 1437 (441) | 1391 (711) | 1428 (866) | 1443 (485) | 1468 (584) | 1472 (722) | 1495 (0.00) | 1491 (445) | 1534 (3) | 1523 (495) | 1528 (0.6) | 1520 (288) | Overlapped | $\nu_{as}(\text{C}=\text{N})$ |
| 1298 (24) | 1291 (5) | 1094 (430) | 1302 (10) | 1113 (406) | 1108 (595) | | | | | | | 1456 | $\delta(\text{N4-H})$ |
| | | | | | | | | | | | | 1216 | $\nu(\text{N4-C5}) + \nu(\text{C}=\text{S}) + \delta(\text{N4-H})$ |

The frequencies are in cm⁻¹ and intensities (in brackets) in km mol⁻¹

^a In CCl₄; ^b Complex mode including $\delta(\text{CO})$

Fig. 3 B3LYP/6-311++G(*d,p*) optimized structures of dimers of tautomers **1B_{rot}** and **2B_{rot}**



2B cannot be ruled out. The amount of this form in acetone and ethanol solution is 2.09 and 2.37 %, respectively.

The results from vibrational energy distribution analyses of the calculated frequencies for the optimized structures of tautomers **A** and **B** for compounds **1** and **2** at the B3LYP/6-311++G(*d,p*) level are given in Tables 3 and 4. The apparent difference in position of predicted C=O and C=N stretching frequencies of tautomers **A** and **B** clearly shows the distinction in bonds conjugation. In tautomer **A** (“conjugated” form) C=O and C=N bonds are conjugated to each other, whereas in tautomer **B** (“non-conjugated” form) they are not (Fig. 1). Thus, the C=N frequency change can be used as a reliable indication for observation of these two tautomers. On the base of such analysis,

Lempert et al. [30] have shown that 2-methylthio-4,4/5,5/-diphenyl-2-imidazolin-5(4)-one exist in solid state in two different tautomeric forms.

The measured C=N stretching vibration at 1579 cm^{−1} in saturated CCl₄ solution (Table 4) clearly shows that compound **1** exists as “non-conjugated” tautomeric form **B** or **B_{rot}** that is in agreement with the results from the quantum chemical calculations listed in Table 2. Probably the tautomeric form **1B_{rot}** is stabilized by a dimeric molecule associate (Fig. 3) by means of intermolecular N–H...O hydrogen bonds. This assumption is confirmed by the presence of two carbonyl frequencies at 1753 and 1723 cm^{−1} in the IR spectrum measured in CCl₄ (see Fig. 4; Table 3) and is in agreement with calculated frequencies in CCl₄ solvent

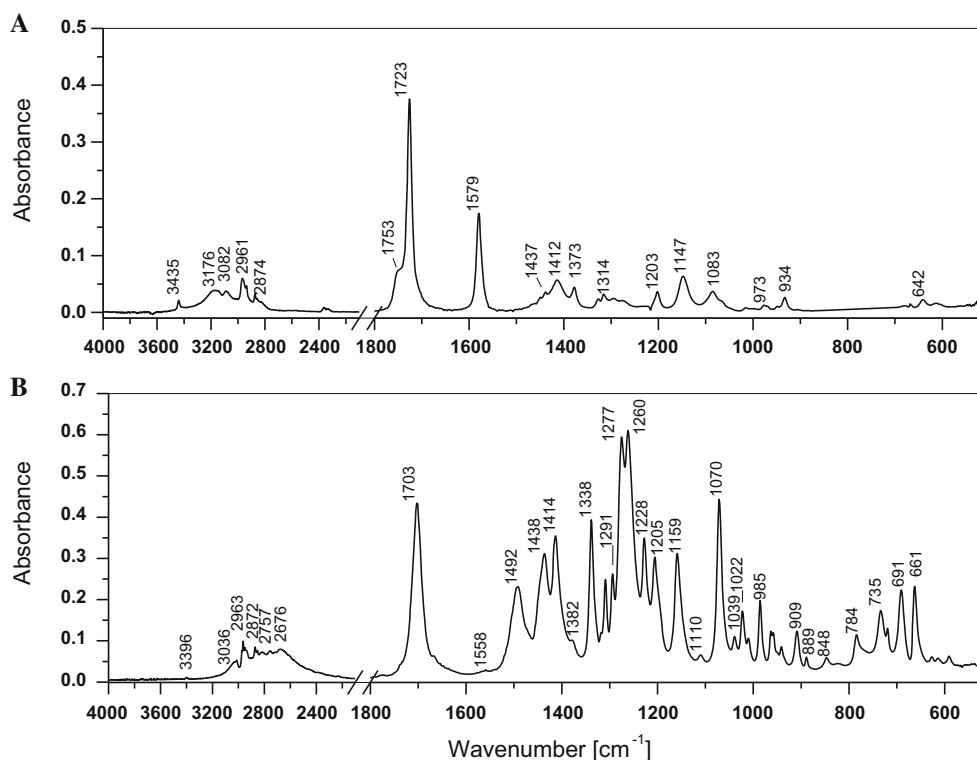


Fig. 4 Infrared spectra of 2-(methylthio)-1,3-diazaspiro[4.4]non-2-ene-4-one (**1**) in: **a** CCl₄ and **b** crystalline powder

Table 5 B3LYP/6-311++G(*d,p*) calculated interatomic distances (Å) for tautomer **A** as isolated molecule (Fig. 1) and in trimer structure (Fig. 8), and for tautomer **B** as isolated molecule (Fig. 1) and in dimer structure (Fig. 3) of compounds **1** and **2**

| Bond | Compound | | X-ray | Bond | Compound | |
|--------|-----------|---------------------|----------|--------|-------------------------|----------------------------------|
| | 1A | 1A in trimer | | | 1B_{rot} | 1B_{rot} in dimer |
| N1–C2 | 1.473 | 1.466 | 1.476(3) | N1–C2 | 1.476 | 1.478 |
| C2–C3 | 1.551 | 1.549 | 1.526(4) | C2–C3 | 1.533 | 1.531 |
| C3–N4 | 1.397 | 1.387 | 1.384(3) | C3–N4 | 1.391 | 1.369 |
| N4–C5 | 1.306 | 1.326 | 1.344(4) | N4–C5 | 1.401 | 1.403 |
| N1–C5 | 1.365 | 1.342 | 1.325(3) | N1–C5 | 1.276 | 1.279 |
| C3–O | 1.208 | 1.215 | 1.215(3) | C3–O | 1.209 | 1.224 |
| N1–H | 1.008 | 1.019 | 0.931 | N1–H | 1.008 | 1.029 |
| C5–S6 | 1.755 | 1.749 | 1.730(3) | C5–S6 | 1.770 | 1.761 |
| S6–C12 | 1.828 | 1.828 | 1.793(3) | S6–C12 | 1.829 | 1.825 |
| | 2A | 2A in trimer | | | 2B | 2B_{rot} in dimer |
| N1–C2 | 1.477 | 1.474 | 1.472(3) | N1–C2 | 1.478 | 1.477 |
| C2–C3 | 1.541 | 1.540 | 1.524(3) | C2–C3 | 1.528 | 1.528 |
| C3–N4 | 1.372 | 1.364 | 1.353(3) | C3–N4 | 1.365 | 1.349 |
| N4–C5 | 1.318 | 1.338 | 1.358(3) | N4–C5 | 1.408 | 1.409 |
| N1–C5 | 1.350 | 1.333 | 1.313(3) | N1–C5 | 1.273 | 1.275 |
| C3–S | 1.649 | 1.657 | 1.658(2) | C3–S | 1.647 | 1.662 |
| N1–H | 1.007 | 1.021 | | N1–H | 1.009 | 1.029 |
| C5–S6 | 1.750 | 1.745 | 1.722(2) | C5–S6 | 1.768 | 1.759 |
| S6–C12 | 1.828 | 1.827 | 1.798(3) | S6–C12 | 1.830 | 1.825 |

The X-ray data for **1** and **2** are given for comparison

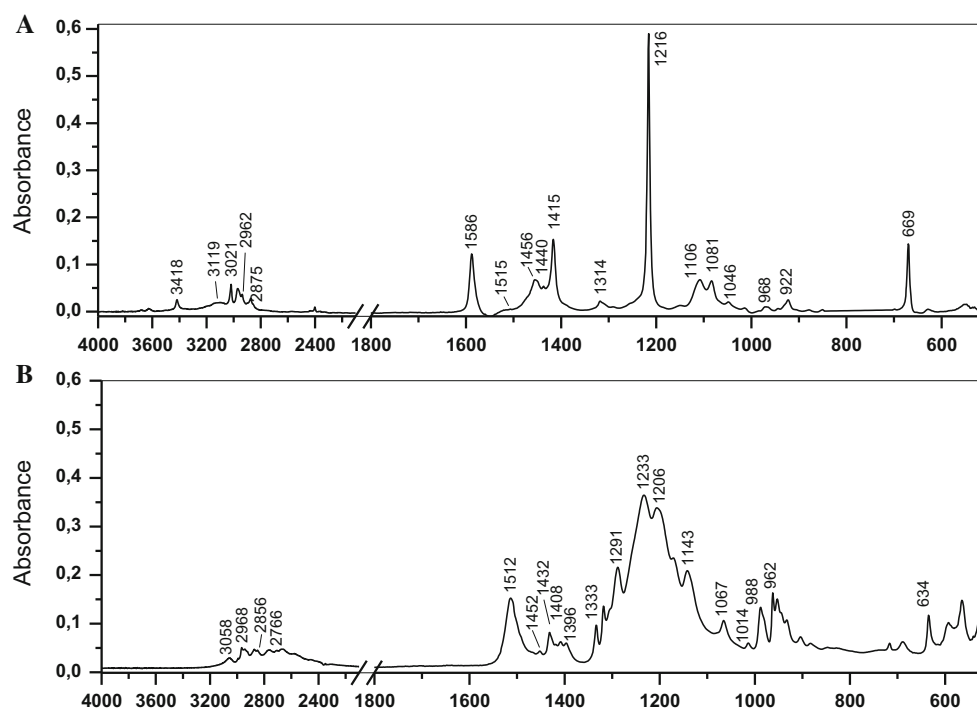


Fig. 5 Infrared spectra of 2-(methylthio)-1,3-diazaspiro[4.4]non-2-ene-4-thione (**2**) in: **a** CCl_4 and **b** crystalline powder

(Table 3). The C=N characteristic band at 1579 cm^{-1} is too broad (Fig. 4). This broadening can be explained by the presence of two closely lying frequency bands, $\nu_{\text{as}}(\text{C}=\text{N}) \sim 1616\text{ cm}^{-1}$ and $\nu_{\text{s}}(\text{C}=\text{N}) \sim 1612\text{ cm}^{-1}$ are predicted. The first one is very intensive, while the second one has low intensity (Table 4). Two N–H characteristic band for the dimer are predicted at 3289 and 3256 cm^{-1} . The first band, $\nu_{\text{as}}(\text{N}–\text{H})$, should be very intensive, while the second one, $\nu_{\text{s}}(\text{N}–\text{H})$, is calculated to be very low intensive (Table 4) and that is why only one N–H band at 3435 cm^{-1} is observed (Fig. 4). As would be expected, there is a certain interaction between $\nu(\text{C}=\text{N})$ and $\delta(\text{N}–\text{H})$ in-plane characteristic vibrations for the secondary amides. However, we must note that the amide II band is absent in the interval $1570\text{--}1530\text{ cm}^{-1}$ in the spectrum of dimers of **B** or **B_{rot}** since this band is not typical for “cis” configuration of carbonyl and NH bonds as in the structures presented in [38]. This significantly simplifies the spectral identification of the $\nu(\text{C}=\text{N})$ position in the respective IR spectra.

The dimer structure of **1B_{rot}–1B_{rot}** is shown in Fig. 3, and geometric parameters for **1B_{rot}** and its dimer, calculated at B3LYP/6-311++G(*d,p*) level, are compared in Table 5. When the dimer is formed, the C3–N4 bonds are shortened by 0.022 Å , while the C3=O and N–H bonds lengthen by 0.015 and 0.021 Å , respectively. All rest bonds almost do not change.

Similar IR spectral features can be observed for compound **2** at the above mentioned experimental conditions (see Fig. 5; Table 4). We have to note that unlike the case of the compound

1 wherein dimeric form predominates, the IR spectrum of **2** in saturated CCl_4 solution indicates clearly that the supposed dimeric form may coexist with the monomeric one (see Fig. 5; Table 3). Similar to compound **1**, in the dimer of compound **2** the C3–N4 bond is shortened by 0.016 Å in comparison with that one in the isolated molecule, and the C3=S and N–H bonds are longer by 0.015 and 0.020 Å , respectively.

As can be seen in the IR spectrum of **1** in ethanol, the band corresponding to the C=N stretch differs in the position for tautomer **A** and **B** (Tables 3, 4). The measured characteristic C=N stretching frequency for **1** is at 1581 and 1571 cm^{-1} (Fig. 6). These frequencies turn out to be very different from predicted values 1439 cm^{-1} for **A** in EtOH, 1462 cm^{-1} for **A_{rot}** (see Table 3) but in the same time are close to those calculated for **B_{rot}** (1611 cm^{-1}) and 1610 cm^{-1} and 1605 cm^{-1} , for its dimer (see Table 4). However, the predicted C=N frequencies for **1A** tautomer (62.08 % see Table 1) cannot be experimentally observed due to the absorption of methylene group of ethanol. Similar result is obtained for compound **2** (Table 4)—**2A**: calculated, 1420 cm^{-1} , and experimental, 1595 cm^{-1} .

Quantum chemically calculated carbonyl frequencies of **1B_{rot}** in ethanol at 1758 cm^{-1} for monomer and doubled at 1730 and 1721 cm^{-1} for its dimer (Table 4) are in good agreement with the experimentally observed modes at 1752 and 1729 cm^{-1} (Fig. 6). The last broad band contains more than one component since it probably contains the C=O bands of the rotamers **1A** (1718 cm^{-1}) and **1A_{rot}** (1728 cm^{-1}) (Table 3).

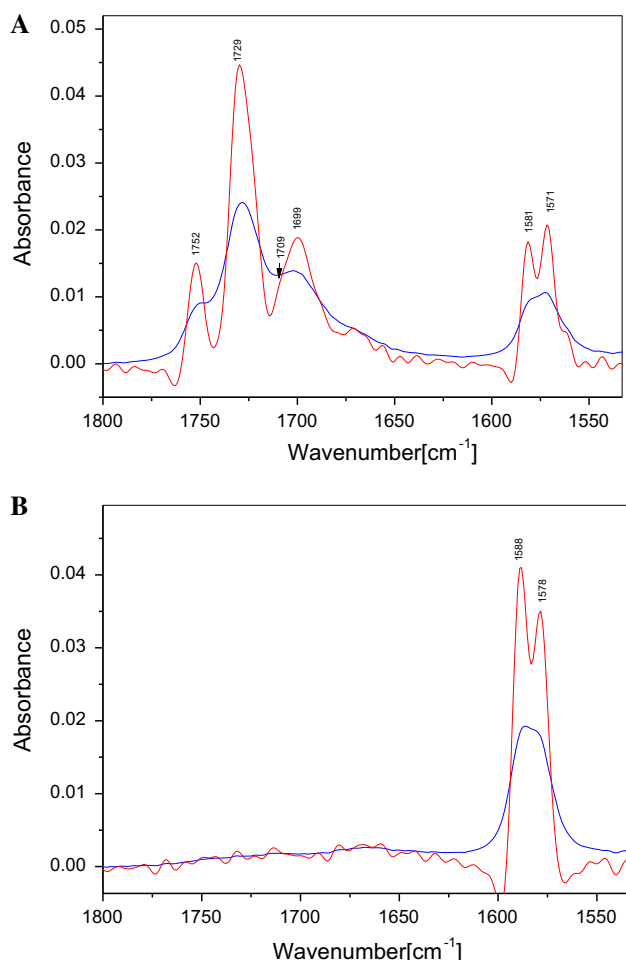


Fig. 6 Infrared spectra of: **a** 2-(methylthio)-1,3-diazaspiro[4.4]non-2-ene-4-one (**1**) and **b** 2-(methylthio)-1,3-diazaspiro[4.4]non-2-ene-4-thione (**2**) in ethanol. Original—in blue; deconvoluted—in red (Color figure online)

Solid-state structure

The two new compounds **1** and **2** were investigated in solid state by single-crystal diffraction, solid-state IR spectra, and solid-state NMR in terms to complete the data.

Both compounds crystallized in monoclinic P21/c space group in similar cells with $Z = 4$ and volumes 884.15(7) and 975.06(7) Å³, respectively. As it can be expected, the volume of compound **2** is slightly bigger, because oxygen atom is substituted with the bigger sulfur atom. All non-hydrogen atoms are fully refined with G. Sheldrick SHELXL software [39] by using Olex2 interface [32]. The equivalent bond lengths and angles in both structures are very similar to each other and show a good agreement with the same type of bonds observed in Cambridge Structural Database (CSD) for the same type of molecular structures. All hydrogen atoms, except the hydrogen atom attached to N1-atom, were automatically assigned by the HFIX command according to the appropriate hybridization. The

determination of the last hydrogen atom is very important for current research. As it was discussed in the beginning, three different tautomers can be observed (Fig. 1). Even that the calculation of the position of hydrogen atoms bound to nitrogen or oxygen is not easy in the case of low-temperature data (in our case 100 K) and Cu X-ray radiation, the hydrogen coordinates can be taken from the list of residual density maxima. For both structures, residual density maxima predicted that hydrogen atom is connected to N1, which means that tautomer **A** was observed as preferred for compounds **1** and **2** in solid state. In agreement with that solution C3=O11 and C3=S11 bond lengths are 1.215(3) and 1.658(2) Å, respectively, which shows double bond behavior in both cases and completely excludes tautomer **C** as possible in solid state. Careful analysis of C–N bonds inside five-member rings (Table 5) shows that N4–C5 and N4–C3 bonds are very similar to each other, showing delocalized double bond behavior probably stabilized by conjugation with C3=O11(S11) double bonds for both crystal structures. In addition, N1–C2 bond lengths, 1.476(3) and 1.472(3) Å for compound **1** and **2**, respectively, are appropriate for single bond between C(*sp*³) and N(*sp*²) atoms. The observed bond lengths, 1.325(3) and 1.313(3) Å, between C5(*sp*²) and N1(*sp*²) atoms are slightly shorter than the expected 1.400 Å for single bond between such atoms, but in reasonable experimental range, which also can be explained by the presence of intramolecular hydrogen bonds, discussed below.

The crystal structure of investigated compounds is presented in Fig. 7. The molecular packing in **1** and **2** is governed by the hydrogen bonding properties of the imidazoline moiety. In both structures the molecules are arranged in long chains in which imidazoline moieties are linked through N–H...N hydrogen bonds (Fig. 7).

We have to note that regardless of the type of solvent (CCl₄, CHCl₃, CH₃COCH₃, or C₂H₅OH) the compounds **1** and **2** are crystallized in solid state forming only a tautomer **A**. Similar result is also obtained by means of a sublimation.

The substantial difference between positions of the characteristic C=N bands in CCl₄ solution and crystalline phase for both compounds (see Figs. 4, 5) suggests that different tautomers exist in solution and in solid state. Unlike the situation in saturated CCl₄ solution, the C=N stretching frequency is shifted to 1492 cm^{−1} in solid state for compound **1** (Fig. 4) and to 1432 cm^{−1} in solid compound **2** (Fig. 5), indicating that tautomer **A** (“conjugated” form) exists in crystalline phase (see Table 3).

Most probably the formation of H-bonding chain between molecules of both compounds in crystalline phase leads to stabilization of the tautomer **A**. This is revealed by a low-frequency shift of carbonyl (1703 cm^{−1}), N–H

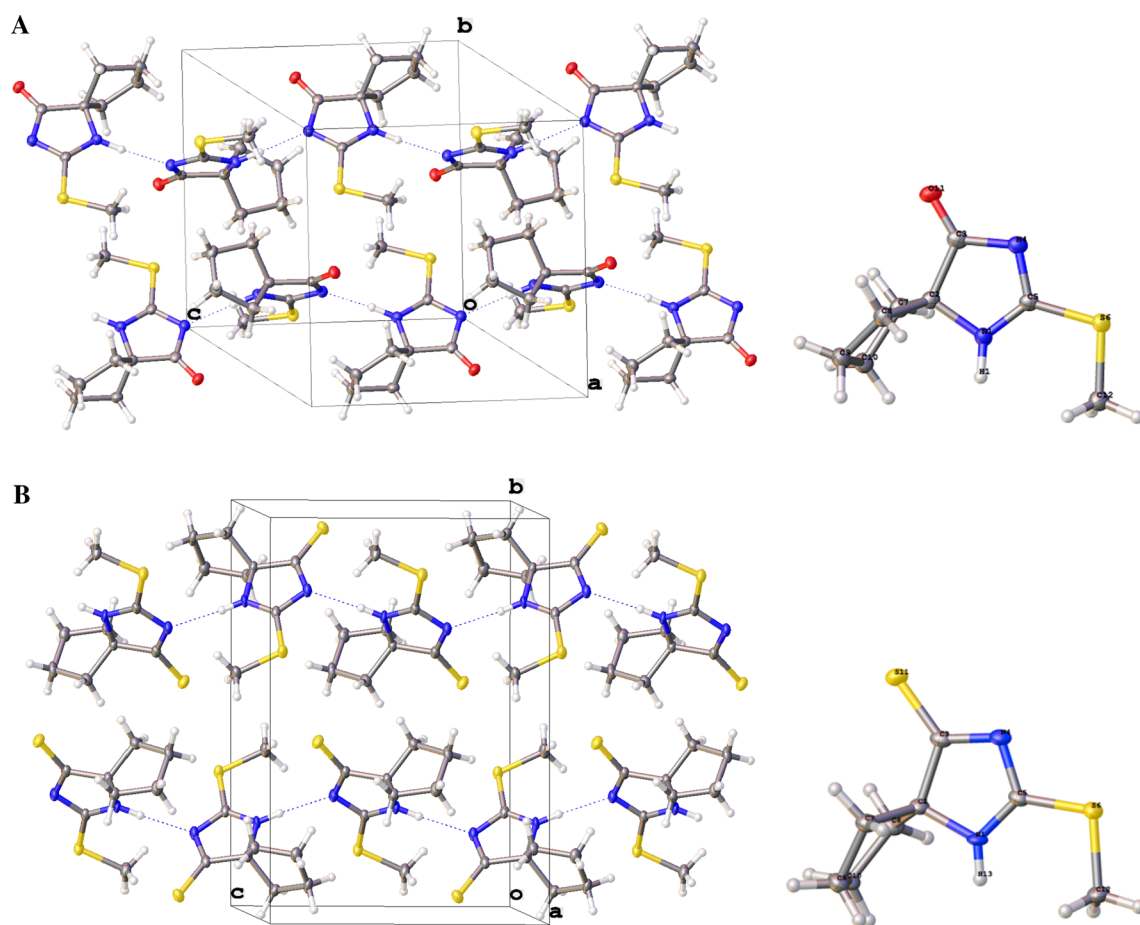


Fig. 7 Cell packing and crystal structure of: **A** 2-(methylthio)-1,3-diazaspiro[4.4]non-2-ene-4-one (**1**) and **B** 2-(methylthio)-1,3-diazaspiro[4.4]non-2-ene-4-thione (**2**). All thermal ellipsoids are presented with 50 % probability

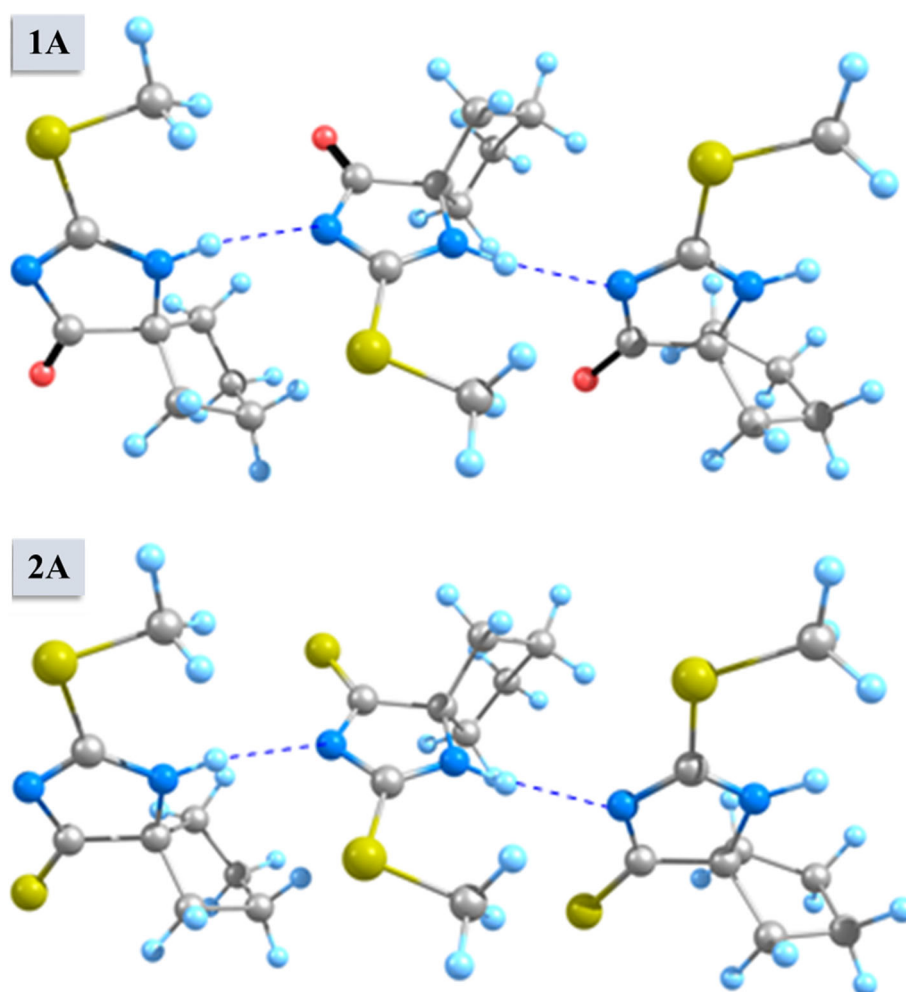
(3396 cm^{-1}) and C=N (1492 cm^{-1}) stretching frequency in the IR solid-state spectra (Fig. 4). Additionally, solid-state spectra become very complex because of the appearance of new spectral bands in C–O–C and C=S frequency regions (see Fig. 5) due to the coupling of vibrational modes in crystalline phase. This is also confirmed by the vibrational mode contribution analysis for the calculated frequencies of compounds **1** and **2** showing that the stretching vibrations of the carbonyl groups and thiocarbonyl group (Table 3) are strongly coupled with the stretching and deformational vibrations of the C–N bonds.

In Table 5 are listed the bond lengths for compounds **1** and **2** derived from the refined crystal structures and compared with those taken from isolated molecule and trimer model (Fig. 8). The quantum chemical calculations are performed at the B3LYP/6-311++G(*d,p*) computational level. In isolated molecule the calculated C3=O (1.208 Å) and N4=C5 (1.306 Å) bond length are shorter, whereas C5–N1 bond (1.365 Å) is longer as compared to those in the X-ray structure (Table 5). The difference

between the calculated and experimental values may be attributed to the intermolecular hydrogen bonding which led to electronic redistribution in the imidazoline ring. That is why trimer models of both compounds were constructed from the crystal structure. The optimized molecular structures of the trimers are shown in Fig. 8, and the bond lengths presented in Table 5 for the trimer are taken from the molecule in the middle.

The bond lengths for the trimer are closer to the experimental values as compared to those for the isolated molecule. It can be seen from Table 5 that significant changes are observed in the bond lengths between the atoms involved in intermolecular interactions. The N4=C5 and N1–H bonds are elongated by 0.020 and 0.011 Å, respectively, while the N1–C5 bond is shortened by 0.023 Å due to N–H...N intermolecular hydrogen bonding in imidazoline moieties of **1**. The B3LYP/6-311++G(*d,p*) calculated N–H...N distance is 2.111 Å, and it differs from that of crystal data. It is due to the crystal forces that give rise to a more packed structure than in our simulation.

Fig. 8 B3LYP/6-311++G(*d,p*) optimized structures of trimers of tautomers **1A** and **2A**



Similar results are obtained for compound **2**. In the trimer the N4=C5 and N1–H bonds are elongated by 0.020 and 0.014 Å, respectively, and the N1–C5 bond is shorter by 0.017 Å, in comparison with the isolated molecule. In this way, taking into account the intermolecular hydrogen bonding, the calculated bond lengths in imidazoline moiety are closer to the X-ray data.

Solid-state NMR spectra

Chemical shifts for ^{13}C and ^{15}N (Fig. 9) were assigned on a base of calculated shielding constants (Table 6). For both compounds the number of resonances in the spectra does not exceed the number of carbon atoms in the molecule, which suggests that there is one molecule in the asymmetric unit cell, in agreement with the crystallographic data. For compound **2** the resonances of C9 and C10 are overlapped giving a broadened signal at 25.8 ppm. Analysis of C3 chemical shift showed that carbonyl group (compound **1**) and thioamide group (compound **2**) are

present in molecular structure, what suggests that tautomer **C** is not observed in the crystals. Theoretical ^{13}C NMR chemical shifts are in good agreement with measured ones, although systematic error is observed and thus all theoretical values are overestimated. In ^{15}N NMR spectra there are two signals arising from N1 and N4 nitrogen atoms. The separation between them is about 65 ppm for compound **1** and 82 ppm for compound **2**. Theoretical calculations of ^{15}N NMR chemical shifts performed for isolated molecules of tautomer **1** revealed large discrepancy between theoretical and measured values. The calculated shift for N1 was underestimated of ca. 50 ppm and for N4 of ca. 20 ppm. These differences indicate that both nitrogen atoms are engaged in intermolecular hydrogen bonds which can have a great impact on ^{15}N NMR chemical shift. Including the network of intermolecular hydrogen bonds into calculations done for trimer significantly improved the theoretical values. The error for N4 atoms was less than 4 ppm, but N1 was still underestimated by about 20 ppm. It can be due to the differences between calculated hydrogen bond geometry and that present in the crystal.

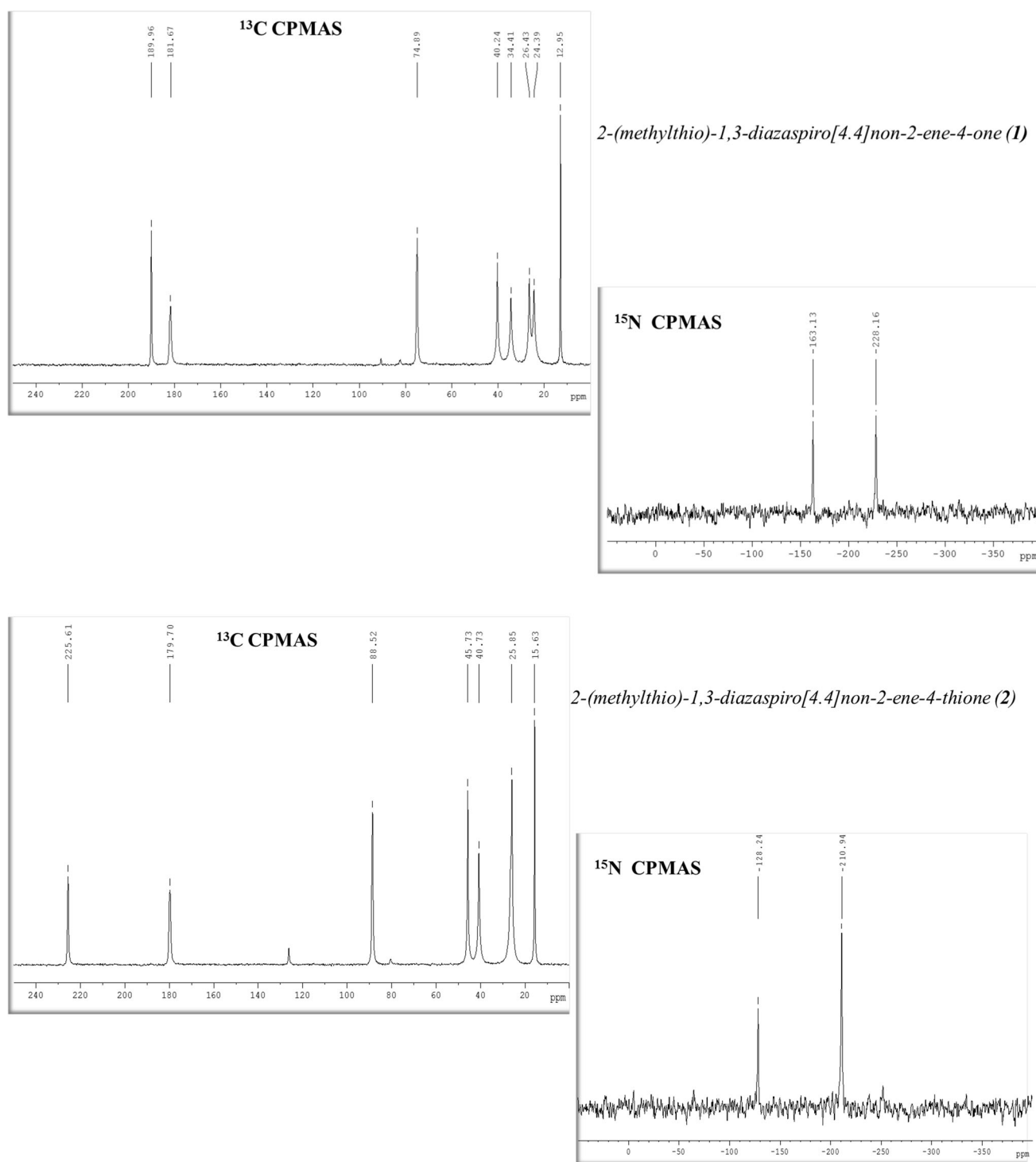


Fig. 9 ¹³C CPMAS and ¹⁵N CPMAS NMR spectra of compounds **1** and **2**

Additionally, the nitrogen atom is especially sensitive [40] to surroundings [41], and it is no surprise that it deviates from experimental values.

The above discussion showed that for both compounds (see Figs. 4, 5) different tautomeric forms **A** and **B** (Fig. 1)

exist at the change of physical state—from solution phase (saturated CCl₄ solution) to the crystalline phase. We suggest to call this phenomenon *desmokatatropy*—from Greeks δεσμός (bond) κατάσταση (state) and τρόπος (change).

Table 6 GIAO ^{15}N and ^{13}C B3LYP/6-311+G(2df,p)//B3LYP/6-311+G(d,p) calculated chemical shifts δ (ppm) for tautomer **A** of compounds **1** and **2** shown on Fig. 1

| Nuclei | Tautomer 1A | | | Tautomer 2A | | |
|--------|--------------------|-----------|--------------|--------------------|-----------|--------------|
| | Calc. | | Experimental | Calc. | | Experimental |
| | Isolated | In trimer | | Isolated | In trimer | |
| N1 | −273.07 | −248.09 | −228.16 | −262.797 | −233.15 | −210.94 |
| C2 | 79.54 | 77.00 | 74.89 | 92.31 | 91.82 | 88.52 |
| C3 | 192.91 | 198.53 | 189.96 | 236.75 | 243.07 | 225.61 |
| N4 | −140.78 | −167.14 | −163.13 | −108.628 | −126.88 | −128.24 |
| C5 | 192.43 | 192.23 | 181.67 | 187.80 | 188.89 | 179.70 |
| C7 | 41.87 | 42.25 | 34.41 | 47.92 | 47.77 | 40.73 |
| C8 | 42.20 | 44.52 | 40.24 | 47.05 | 50.09 | 45.73 |
| C9 | 26.39 | 32.11 | 24.39 | 27.68 | 31.99 | 25.85 |
| C10 | 28.01 | 32.70 | 26.43 | 26.66 | 33.14 | 25.85 |
| C12 | 17.56 | 18.89 | 12.95 | 18.25 | 19.50 | 15.63 |

The atom numbering is shown on Fig. 2

Conclusions

Two new compounds—2-(methylthio)-1,3-diazaspiro[4.4]non-2-ene-4-one, **1**, and 2-(methyl-thio)-1,3-diazaspiro[4.4]non-2-ene-4-thione **2**, are synthesized. The substantial difference between maximum positions of the characteristic C=N band in the IR spectra for both compounds in nonpolar solvent and crystalline phase suggests that in solid state a “conjugated tautomeric form” **A** exists, while in nonpolar solution phase there is “non-conjugated tautomeric form” **B**. The tautomeric equilibria of compounds **1** and **2** are strongly solvent dependent. The compounds exist as a mixture of tautomers **1A**, **1A_{rot}**, and **1B_{rot}** in weakly polar (CHCl_3) and polar (acetone and ethanol) solvents.

At change of physical state, from nonpolar solution phase to the crystalline phase, different tautomeric forms exist. It is suggested to call this phenomenon *desmokatatropy*.

Supporting information

Supporting information (SI) is available and it contains: Tables of absolute energies of the tautomers and rotamers of **1** and **2** (Tables 1S–3S) and their atom coordinates.

Full details of the crystal structure determination in CIF format are available. The crystal structures of 2-(methylthio)-1,3-diazaspiro[4.4]non-2-ene-4-one (**1**) and 2-(methylthio)-1,3-diazaspiro[4.4]non-2-ene-4-thione (**2**) have been deposited in CCDC (CCDC 1495035–1495036).

Acknowledgments The calculations were performed on the computer system installed at the Institute of Organic Chemistry, Bulgarian Academy of Sciences with the financial support of the National Science Fund, Project “MADARA” (Grant DO 02-52/2008). The authors also thank the generous funding from NSF-CRIF (CHE-

0946990) for the purchase of XRD instrumentation at Chemistry and Biochemistry Department, North Dakota State University.

References

- Geuther A (1863) Arch Pharm 166:97–110
- Baeyer A, Oekonomides S (1882) Ber Dtsch Chem Ges 15:2093–2102
- Baeyer A (1883) Ber Dtsch Chem Ges 16:2188–2204
- Laar C (1885) Ber Dtsch Chem Ges 18:648–657
- Jacobson P (1887) Ber Dtsch Chem Ges 20:1895–1903
- Hantzsch A, Hermann F (1887) Ber Dtsch Chem Ges 20:2801–2811
- Claisen L (1896) Liebigs Ann Chem 291:25–137
- Lowry TM (1914) Proc Chem Soc 30:105–107
- Oppe A (1914) Jahrb Radioakt Elektron 10:368–405
- Gawinecki R, Kolehmainen E, Osmialowski B, Palkovic P, Nissinen M (1999) Heterocycl Commun 5:549–551
- Gawinecki R, Osmialowski B, Kolehmainen E, Nissinen M (2000) J Mol Struct 525:233–239
- García MA, López C, Claramunt RM, Kenz A, Pierrot M, Elguero J (2002) Helv Chim Acta 85:2763–2776
- Elguero J (2011) J Cryst Growth Des 11:4731–4738 (references therein)
- Cruz-Cabeza AJ, Groom CR (2011) Cryst Eng Comm 13:93–98
- Kubicki M (2004) Acta Crystallogr B 60:191–196
- Song J, Mishima M, Rappoport Z (2007) Org Lett 9:4307–4310
- Wu ZH, Ma JP, Wu XW, Huang RQ, Dong YB (2009) Acta Crystallogr C Cryst Struct Commun 65:o128–o130
- Enchev V, Angelova S, Rogojerov M, Monev V, Wawer I, Tkaczyk M, Kostova K (2011) J Phys Chem A 115:2026–2034
- Steiner T, Koellner G (1997) Chem Commun (13):1207–1208
- Pizzala H, Carles M, Stone WEE, Thevand A (2000) J Mol Struct 526:261–268
- Bechtel F, Gaultier J, Hauw C (1973) Cryst Struct Commun 2:469–472
- Bhatt PM, Desiraju GR (2007) Chem Commun (20):2057–2059
- Enchev V, Abrahams I, Angelova S, Ivanova G (2005) J Mol Struct Theochem 719:169–175
- Rubčić M, Užarević K, Halasz I, Bregović N, Mališ M, Dilović I, Kokan Z, Stein RS, Dinnebier RE, Tomišić V (2012) Chem Eur J 18:5620–5631

25. Chierotti MR, Ferrero L, Garino N, Gobetto R, Pellegrino L, Braga D, Grepioni F, Maini L (2010) *Chem Eur J* 16:4347–4358
26. Schmidt MU, Brüning J, Glönnemann J, Hützler MW, Mörschel P, Ivashevskaya SN, Van De Streek J, Braga D, Maini L, Chierotti MR, Gobetto R (2011) *Angew Chem* 123:8070–8072
27. Martin YC (2009) *J Comput Aided Mol Des* 23:693–704
28. Faller B, Ertl P (2007) *Adv Drug Deliv Rev* 59:533–545
29. Sala LF, Martell AE, Motekaitis RJ, Abbott H (1987) *Inorg Chim Acta* 135:123–127
30. Lempert K, Nyitrai J, Sohár P, Zauer K (1964) *Tetrahedron Lett* 5:2679–2684
31. Lempert K, Nyitrai J, Zauer K, Kálmán A, Argay G, Duisenberg AJM, Sohár P (1973) *Tetrahedron* 29:3565–3569
32. Dolomanov OV, Bourhis LJ, Gildea RJ, Howard JAK, Puschmann H (2009) *J Appl Cryst* 42:339–341
33. Schmidt MW, Baldrige KK, Boatz JA, Elbert ST, Gordon MS, Jensen JH, Koseki S, Matsunaga N, Nguyen KA, Su S, Windus TL, Dupuis M, Montgomery JA Jr (1993) *J Comput Chem* 14:1347–1363
34. Gordon MS, Schmidt MW (2005) In: Frenking G, Kim KS, Scuseria GE, Dykstra CE (eds) *Theory and applications of computational chemistry: the first forty years*. Elsevier, Amsterdam, pp 1167–1189
35. Cossi M, Rega N, Scalmani G, Barone V (2003) *J Comput Chem* 24:669–681
36. Boys SF, Bernardi F (1970) *Mol Phys* 19:553–566
37. Frisch MJ, Trucks GW, Schlegel HB, Scuseria GE, Robb MA, Cheeseman JR, Scalmani G, Barone V, Mennucci B, Petersson GA, Nakatsuji H, Caricato M, Li X, Hratchian HP, Izmaylov AF, Bloino J, Zheng G, Sonnenberg JL, Hada M, Ehara M, Toyota K, Fukuda R, Hasegawa J, Ishida M, Nakajima T, Honda Y, Kitao O, Nakai H, Vreven T, Montgomery JA Jr, Peralta JE, Ogliaro F, Bearpark M, Heyd JJ, Brothers E, Kudin KN, Staroverov VN, Kobayashi R, Normand J, Raghavachari K, Rendell A, Burant JC, Iyengar SS, Tomasi J, Cossi M, Rega N, Millam JM, Klene M, Knox JE, Cross JB, Bakken V, Adamo C, Jaramillo J, Gomperts R, Stratmann RE, Yazyev O, Austin AJ, Cammi R, Pomelli C, Ochterski JW, Martin RL, Morokuma K, Zakrzewski VG, Voth GA, Salvador P, Dannenberg JJ, Dapprich S, Daniels AD, Farkas Ö, Foresman JB, Ortiz JV, Cioslowski J, Fox DJ (2009) In: *Gaussian, Inc., Wallingford, CT*
38. Stuart BH (2004) *Infrared spectroscopy: fundamentals and applications*. Wiley Ltd., London
39. Sheldrick G (2008) *Acta Cryst A* 64:112–122
40. Barfield M, Fagerness P (1997) *J Am Chem Soc* 119:8699–8711
41. Osmialowski B, Kolehmainen E, Dobosz R, Gawinecki R, Kauppinen R, Valkonen A, Koivukorpi J, Rissanen K (2010) *J Phys Chem A* 114:10421–10426